Published in final edited form as:
Nanomedicine. 2013 April ; 9(3): 419–427. doi:10.1016/j.nano.2012.09.003.

Cell penetrating peptides released from thermosensitive nanoparticles suppress proinflammatory cytokine response by specifically targeting inflamed cartilage explants

Rush L Bartlett II[#], **Shaili Sharma**[#], and **Alyssa Panitch**[*]
Weldon School of Biomedical Engineering, Purdue University, 206 S. Martin Jischke Drive, West Lafayette Indiana, 47907

[#] These authors contributed equally to this work.

Abstract

Cell penetrating anti-inflammatory peptide KAFAKLAARLYRKALARQLGVAA (KAFAK) has the ability to suppress pro-inflammatory cytokines TNF-α and IL-6 when released from degradable and non-degradable Poly(NIPAm-AMPS) nanoparticles. *In vitro* human macrophage model with THP1 human monocytes and *ex vivo* bovine knee cartilage tissue both showed a dose dependent suppression of pro-inflammatory cytokines when treated with KAFAK loaded poly(NIPAm-AMPS) nanoparticles. When bovine knee cartilage explants were treated with KAFAK loaded poly(NIPAm-AMPS) nanoparticles, rapid and highly selective targeting of only damaged tissue occurred. This study has demonstrated selective targeting and therapeutic efficacy of KAFAK when released from both degradable and non degradable poly(NIPAm-AMPS) nanoparticles in *in vitro* and *ex vivo* models. As a result, poly(NIPAm-AMPS) nanoparticles loaded with KAFAK could a very effective tool to treat osteoarthritis.

Keywords

Cell penetrating peptides; thermosensitive polymer; osteoarthritis

Background

Thermosensitive polymer poly(N-isopropylacrylamide), abbreviated poly(NIPAm), has been extensively studied due to a physiologically relevant lower critical solution temperature (LCST) between 31–33°C. The LCST allows the polymer to form a solution when exposed

[*]Author to whom correspondence should be addressed Fax: +1 765-496-1459.Phone: +1 765 496-1313.

Conflict of interest: Moerae Matrix, Inc. holds an exclusive worldwide license to the MK2 inhibitor technology. Dr. Panitch owns greater than a 10% interest in Moerae Matrix, Inc.

Rapid and selective targeting specific to diseased tissue can be achieved using thermosensitive nanoparticles loaded with cell penetrating anti-inflammatory peptides.

to an aqueous environment at temperatures below 31°C and phase separates under physiological conditions. Solubilization at room temperature results in swelling of nanoparticles composed of crosslinked poly(NIPam), that facilitates rapid loading of aqueous soluble, degradation sensitive therapeutics by passive diffusion. Charged carboxylic acid co-monomers, such as acrylic acid, are traditionally added to poly(NIPAm) nanoparticles in order to increase colloidal stability and provide a secondary site for chemical modification. In addition to carboxylic co-monomers, Garcia et el. have shown that it is possible to incorporate sulfated co-monomer, 2-acrylamido-2-methyl-1-propanesulfonic acid (AMPS), into poly(NIPAm) nanoparticles. Previous work in our laboratory has demonstrated that the copolymerization of AMPS and NIPAm to form poly(NIPAm-co-AMPS) nanoparticles greatly enhances the electrostatic attraction between cationic cell penetrating peptides (CPPs) and the anionic nanoparticles, which results in increased drug loading.

Anti-inflammatory CPPs under investigation by our laboratory target mitogen activated protein kinase activate protein kinase 2 (MK2) to reduce expression of pro-inflammatory cytokines. As a member of the p38 mitogen activated protein kinase pathway, MK2 controls expression of many pro-inflammatory cytokines such as, but not limited to, IL-1, TNF-α, and IL-6. MK2's key role involves activation of transcription factors that affect the stability of cytokine AU rich mRNA. This pathway is triggered by the presence of pro-inflammatory cytokines, fragmented extracellular matrix materials, or exogenous antigens. Our laboratory has previously developed a promising MK2 inhibiting, cell penetrating peptide with the amino acid sequence KAFAKLAARLYRKALARQLGVAA (abbreviated KAFAK). However, in order to be useful in a therapeutic setting, a tailored delivery system that protects the peptide from enzymatic degradation, and thus increases the half-life of the peptide therapeutic, is needed.

In the study reported here, we examined the ability of poly(NIPAm-co-AMPS) to release CPP KAFAK to suppress inflammation in a lipopolysaccharide (LPS) induced, *in vitro*, inflammatory model and an interlukin-1 beta (IL-1β) induced, *ex vivo*, inflammatory model. We hypothesized that these drug-loaded particles could be specifically delivered to inflamed sites to suppress expression of pro inflammatory cytokines in inflamed tissue matrices, such as articular cartilage. Cytokines including IL-1β and tumor necrosis factor-α (TNF-α) initiate the inflammatory cascade for several diseases, including osteoarthritis (OA). During the progression of OA, chondrocytes synthesize proteolytic enzymes in response to pro inflammatory cytokines and degrade key extracellular matrix components. Aggrecan, a proteoglycan that serves to protect cartilage matrix by hindering diffusion of cytokines and proteolytic enzymes, is usually the first component to undergo degradation. In this study we simulate the first stages of OA by removing native aggrecan from a bovine cartilage explant and entice chondrocytes to produce cytokines and proteolytic enzymes by stimulating with IL-1β. Our results indicate the ability of poly(NIPAm-AMPS) nanoparticles to selectively diffuse through degraded cartilage explants and the loaded KAFAK to significantly suppress cytokine production. These results suggest that this nanoparticle-peptide combination maybe a promising system for inter articular therapies.

Materials & Methods

Chemicals

N-isopropylacrylamide (NIPAm) was acquired from Polysciences Inc. (Warrington, PA, USA). N,N'-methylenebisacrylamide (MBA), sodium dodecyl sulfate (SDS; 10% w/v in water), 2-acrylamido-2-methyl-1-propanesulfonic acid (AMPSA), and potassium persulfate were acquired from Sigma-Aldrich (St. Louis, MO, USA). NIPAm, MBA, and AMPSA were stored under nitrogen at 4°C. All water used in synthesis, dialysis, and testing was treated by a MilliQ system (Millipore, Billerica, MA, USA; 18.2 MΩ·cm resistivity).

DMHA Synthesis

N,O-dimethacryloylhydroxylamine (DMHA) was synthesized according to methods previously reported by Ulbrich et. al. Briefly, 10.1 g of hydroxylamine (VWR International, Radnor, PA, USA) was dissolved in 50 ml pyridine (Mallinckrodt Chemicals, St. Louis, MO, USA) followed by 25.4 g of methacryloyl chloride (Alfa Aesar, Ward Hill, MA, USA) added drop wise in an ice bath. The methacryloyl chloride was allowed to react for 20 minutes at 4°C after which the reaction was continued at room temperature for 4 hours. The reaction was neutralized with 21 ml of concentrated HCL (Sigma-Aldrich) and dissolved in 100 ml Chloroform (Honeywell, Morristown, NJ, USA). The product was washed with four 150 ml washes of MilliQ water and the organic layer was separated and dried over anhydrous $MgSO_4$ (Mallinckrodt Chemicals). Chloroform was evaporated in a vacuum and the product was dissolved in diethyl ether (Mallinckrodt Chemicals). Heptane (VWR International) was slowly added until a crystalline compound was precipitated. Yield (24%); melting point: 54–56°C; Purity and composition were confirmed by using a Varian Unity 300 MHz NMR spectrometer at the Purdue Core NMR Facility.

Nanogel Synthesis

NIPAm-containing nanogels were synthesized using standard precipitation polymerization. Briefly, the nanogel compositions described in Table 1 were formed by dissolving 768.5 mg NIPAm, MBA if required, and AMPSA in 30 ml degassed MilliQ water in a three neck round bottom flask. If DMHA was required it was pre-dissolved in 10 ml of dimethyl sulfoxide (DMSO). If DMHA was not required 10 ml of DMSO was added to the reaction flask after 5 minutes. After addition of the DMHA or DMSO alone, 575 μl of a 10% SDS in MilliQ water solution were added, and the mixture was heated to 75°C under nitrogen. 33.7 mg of potassium persulfate was dissolved in 10 ml degassed MilliQ water and added after 30 minutes equilibration to initiate polymerization. After 4 hours, the reaction was removed from heat and allowed to cool to room temperature. Particles were dialyzed against MilliQ water for 7 days using a 15,000 MWCO membrane. Post dialysis concentrations varied between 6–15 mg/ml and were diluted or concentrated as necessary through lyophilzation and resuspension. To lyophilize nanoparticle, solutions were frozen to −80°C for 12 hours and then placed under lyophilizer vacuum until the liquid was removed.

Nanogel Characterization

After calibration with polystyrene beads a Nano-ZS90 Zetasizer (Malvern, Westborough, MA, USA) was used to measure nanoparticle diameter through dynamic light scattering (DLS). Samples were equilibrated for 2 minutes for each half-degree temperature change for a temperature sweep or 5 minutes for a static temperature measurement. Zeta (ζ) potentials were measured at 23°C by a Nano-ZS90 Zetasizer in folded capillary cells in MilliQ water. TEM was conducted at the Purdue University Life Science Microscope Facility on a FEI/ Philips CM-100 Transmission Electron Microscope at 100 KV using an uranyl acetate stain (UA) at pH 4.5. Discharged TEM sample grids were placed onto the top of a droplet of sample for 2 minutes. Then UA stain was added and samples were briefly dried before imaging at room temperature.

Peptide Synthesis and Purification

Therapeutic peptides were synthesized using 9-fluorenylmethyloxycarbonyl (FMOC) chemistry on Knorr-amine resin (Synbiosci Corp, Livermore, CA, USA). Two coupling steps were used to attach amino acids (Synbiosci Corp). For the first coupling, N-hydroxybenzotriazole (HoBt) and N, N'- diisopropylcarbodiimide (DIC) were incubated with amino acid and resin for 30 minutes. The second 30-minute coupling used 2-(1Hbenzotriazole-1-yl)-1,1,3,3-tetramethyluronium hexafluorophosphate (HBTU), lutidine, and amino acid to increase yield. Peptides were cleaved with a cocktail of trifluoroacetic acid (Sigma-Aldrich), triisopropyl silane (TCI America, Boston, MA, USA), ethane dithiol (Alfa Asara, Ward Hill, Massachusetts, USA), and MilliQ water. Peptide was immediately precipitated in ether, recovered by centrifugation, solubilized in MilliQ water, and lyophilized. Peptides were purified on a FPLC AKTA Explorer (GE Healthcare, Pittsburgh, PA, USA) with a 22/250 C18 prep-scale column (Grace Davidson, Deerfield, Illinois, USA) and an acetonitrile gradient with 0.1 % trifluoroacetic acid. Peptide molecular weight was confirmed by matrix-assisted laser desorption ionization time of flight (MALDI TOF) mass spectrometry with a 4800 Plus MALDI TOF/TOF Analyzer (Applied Biosystems, Foster City, CA, USA).

Drug Loading into Nanoparticles

Purified peptide was first dissolved in MilliQ water to create a 30 mg/ml loading solution. Then this solution was added to 60 mg lyophilized nanoparticles with 5% AMPS and varying amounts of crosslinker. Then, the drug-nanoparticle loading solution complex was allowed to incubate for 24 hours at 4°C in the swollen state. After incubation 9 ml of MilliQ water was added and particles underwent 1 hour of centrifugation at 35,000 rpm and 37°C in an Optima L-90k Ultracentrifuge (Beckman Coulter, Indianapolis, IN, USA). Nanoparticle pellet was briefly re-suspended in 2 ml MilliQ water and was lyophilized. Loaded nanoparticles were suspended in sterile PBS or media (Invitrogen, Grand Island, NY, USA) at required concentrations. Measurement of free peptide released into the solution and the amount of peptide loaded was determined using fluorescence analysis with a fluoraldehyde o-phthalaldehyde (OPA) solution (Thermo Scientific, Waltham MA, USA). Images of particles containing fluorescein isothiocyanate (FITC) labeled peptides were taken with an Olympus FV1000 confocal microscope.

THP1 Macrophage Cell Culture

Immortalized human monocytes (THP-1, ATCC, Manassas, VA, USA) were grown in RPMI 1640 with L-glutamine (Mediatech Inc, Manassas, VA, USA) supplemented with 0.05 mM β-mercaptoethanol (Sigma-Aldrich), 10 mM HEPES (Mediatech Inc), 1 mM sodium pyruvate (Mediatech Inc), 10% fetal bovine serum (Thermo Scientific) and 1% penicillin/streptomycin (Mediatech Inc). Cells were used between passage numbers 4 and 8 and maintained at 37°C with 5% CO_2.

In vitro Inflammatory Macrophage model

THP-1 cells were seeded at a density of 200,000 cells/ml and treated with 10 ng/ml phorbol 12-myristate 13-acetate (PMA) (Sigma-Aldrich) for 48 hours to cause differentiation (confirmed by the monocytes becoming adherent). Different concentrations of nanoparticles that had been released after four days of incubation in PBS (pH 7.4, 37°C) were added to the cell culture. The culture was treated with 50 ng/mL of lipopolysaccharide (LPS) (Sigma-Aldrich) for six hours to induce production of TNF-α. During this incubation different concentrations of KAFAK only in PBS (Sigma-Aldrich), and different concentrations of nanoparticles in PBS with KAFAK (Sigma-Aldrich) were also added. PBS and LPS were used as positive and negative controls. After 6 h incubation in the cell culture incubator, the supernatant was collected and stored at −80°C until cytokine analysis could be performed. The number of live cells was determined using the CellTiter 96 AQueous One Proliferation Assay Reagent (Promega, Madison, WI, USA). 20 μl of reagent was added directly to 100 μl of cells and media. After 2 h of incubation in the cell culture incubator, the absorbance was read at 490 nm with a correction at 650 nm.

Chondrocyte Isolation and Culture

Primary chondrocytes were harvested from three-month-old bovine knee joints obtained from an abattoir within 24 hours of slaughter (Dutch Valley Veal, South Holland, IL, USA). Cartilage slices, 150–200 μm thick were shaved from the lateral femoral condyle and washed three times in serum free DMEM medium (50 μg/mL ascorbic acid 2-phosphate, 100 μg/mL sodium pyruvate, 0.1% bovine serum albumin, 100 units/mL penicillin, 100 μg/mL streptomycin and 25 mM HEPES) prior to digestion with 3% fetal bovine serum (FBS) and 0.2% collagenase-P (Roche, Indianapolis, IN, USA) at 37°C for six hours. Released chondrocytes were filtered through 70 μm cell strainer and centrifuged at 1000 rpm three times for five minutes each in medium listed above supplemented with 10% FBS. The cell pellet was re-suspended in 10% FBS supplemented media and plated at 10,000 cells/mL cell density in a 37 °C, 5% CO_2 humidified incubator until confluent. Cells were used between passage 2 and 4 and seeded at 100,000 cells/ml for experiment. To test the effect of nanoparticles and KAFAK on chondrocyte viability, treatments of nanoparticles and KAFAK were added to chondrocytes and incubated for 6 hours. The number of live cells after 6 hours was determined using the CellTiter 96 AQueous One Proliferation Assay Reagent (Promega, Madison, WI, USA). 20 μl of reagent was added directly to 100 μl of cells and media. After 2 h of incubation in the cell culture incubator, the absorbance was read at 490 nm with a correction at 650 nm.

Ex Vivo Inflammatory Model

Cartilage plugs were obtained from three month old bovine knee joints obtained from an abattoir within 24 hours of slaughter (Dutch Valley Veal, South Holland, IL, USA). The plugs were removed from the load-bearing region of the femoral condyle using a 3 mm diameter cork borer. They were then washed three times in serum free medium and equilibrated for three days in 5 % FBS supplemented media. OA like conditions were simulated by removal of native aggrecan using a previously described protocol. Briefly, plugs were treated with 0.5% (w/v) trypsin in HBSS for 3 hours at 37°C to remove aggrecan. After trypsin treatment plugs were washed three times in HBSS and incubated with 20% FBS for 20 minutes to inactivate residual trypsin activity. Inflammation was initiated in the plugs by treating with 20 ng/mL Il-1β. Nanoparticle treatments as specified in Table 2, were added after day two of culture. Fresh IL-1β and nanoparticles were added every two days for an eight-day culture period. Media aliquots were collected and stored in low-bind tubes at −80°C until further analysis.

Analysis of TNF- α in Human Macrophages

TNF-α production was determined with a human ELISA development kit (Peprotech, Rocky Hill, NJ). Capture antibody diluted in PBS was coated overnight onto Nunc MaxiSorp 96-well plates. The plate was washed with sterile filtered PBS four times and then incubated for one hour with blocking buffer containing 1 % bovine serum albumin (Sera Life Sciences, Milford, MA) in PBS. After incubation with blocking buffer the plate was washed with sterile filtered PBS four times. Then samples and standards were added and incubated in the plate with gentle shaking for 2 hours. Samples were PBS washed, plates were incubated with a detection antibody dissolved in PBS for one hour, washed again, and incubated with avidin-horse radish peroxidase conjugate for 30 minutes. The samples were developed by adding 2,2′-azino-bis(3-ethylbenzthiazoline-6-sulphonic acid) (ABTS) liquid substrate (Sigma-Aldrich) and read on absorbance plate reader at 405 nm with a correction at 650 nm. TNF-α production was analyzed at 25 minutes. TNF-α was normalized to cell number with CellTiter data. A student's t-test was used to determine statistical significance.

Confocal Analysis of Nanoparticles in Bovine Knee Plugs

Bovine cartilage plugs were either trypsin treated to simulate OA-like conditions or left in cell culture media to maintain healthy tissue-like environment. Treatments of nanoparticles loaded with FITC labeled KAFAK were re-suspended at 0.5 mg/ml concentration in PBS. Control treatment of FITC KAFAK only was re-suspended at 0.15 mg/ml concentration. Diffusion through the plug was carried out by pipetting 10 μL of treatment or control solution onto articular surface every ten minutes for one hour. Excess solution was removed prior to next treatment. After the last treatment, plugs were incubated for 1 hour at 37°C and washed with 1X PBS three times. A mid sagittal cut was made through the plug to examine diffusion into the plugs from the top edge. Diffusion of FITC KAFAK was monitored using a 488 nm laser excitation on a confocal microscope (Olympus IX81) at 23°C. Fluorescent intensity was quantified using Image J. Intensity in three independent areas in the top and bottom panel of each image was measured. Values represent Average ± SEM.

Analysis of IL-6 in Bovine Knee *Ex Vivo* Model

IL-6 production was determined with a bovine IL-6 ELISA development kit (Thermo Scientific, Rockford, IL, USA). Capture antibody was coated overnight onto Nunc MaxiSorp 96-well plates. The plate was washed and incubated for one hour with 5% sucrose and 4% bovine serum albumin (Sera Life Sciences, Milford, MA) in PBS solution. After washing blocking buffer away, samples and standards were incubated with gentle shaking for one hour. After washing the samples, plates were incubated with a detection antibody for one hour, washed, and incubated with Streptavidin-HRP for 30 minutes. The samples were developed by adding 3,3',5,5'-tetramethylbenzidine (TMB) liquid substrate for 20 minutes before adding a 0.16 M sulfuric acid stop solution. The plate was read on an absorbance plate reader at 450 nm with a correction at 550 nm. IL-6 production was normalized to individual plug weight and to the negative control where plugs with intact aggrecan were IL-1β stimulated. A student's t test was used to determine statistical significance.

Results

The clinical need for a long-term and effective treatment for inflammation of the joint has driven us to study the effects of poly(NIPAM-AMPS) nanoparticles as possible drug delivery vehicles. These polymeric nanoparticles form colloidal structures in water. Adjustments to reaction conditions can produce nanoparticles with sizes ranging between 100 nm and 400 nm in solution (Table 2). Utilizing 5% AMPS co-monomer content produces particles with spherical shape that do not readily aggregate and are capable of delivering therapeutic peptides. The TEM micrographs collected from previous work by our group demonstrate that particles containing 5% AMPS form spherical nanoparticles when cross-linked with MBA or DMHA. Incorporation of MBA produces nanoparticles that do not degrade under physiologically relevant temperature and pH. However, incorporation of DMHA yields a pH sensitive nanoparticle that hydrolytically degrades above pH 5.0.

Incorporation of AMPS into the nanoparticles yielded increased zeta potential and increased drug loading of cell penetrating peptide KAFAK. Table 2 demonstrates that varying the molar concentration of AMPS contained within nanoparticle formulations has a direct impact on the amount of drug that can be passively loaded into the nanoparticles. Passive drug loading by diffusion can be easily achieved at temperatures below 30°C with poly(NIPAm-AMPS) nanoparticles due to particle swelling at temperatures below the LCST.

Below the LCST, particles swell by a factor of 1.2 to 2.2. This variation in swelling at lower temperature is directly related to incorporation of AMPS; increased AMPS incorporation leads to decreased swelling ratios due to some charge repulsion in the collapsed state. Also noted from Table 2, exposure to any of the nanoparticle formulations tested *in vitro* did not yield a statistically significant difference in the viability of chondrocytes or macrophages, two key cell types involved in osteoarthritis.

Previously we demonstrated that poly(NIPAm-co-AMPS) nanoparticles offer some protection to KAFAK from serum proteases, thus enabling the extended release of therapeutically active KAFAK to suppress TNF-α production in macrophages. However,

this effect is only temporary as KAFAK will degrade over time once released. Figure 1 demonstrates a drug release profile conducted in a 10% FBS in PBS environment at 37°C in order to determine the physiologically relevant release profile. Figure 1 demonstrates that nanoparticles without AMPS, as well as fully degradable nanoparticles, rapidly release KAFAK throughout a 24-hour period, and show little to no release at later time points. For the nondegradable particles, this is most likely due to the previously reported observation that KAFAK is not able to completely diffuse out of the collapsed poly(NIPAm-MBA-AMPS) non-degradable nanoparticle systems. Thus, after 24 hours, most of the peptide that can diffuse from the collapsed particles has done so. In the case of the fully degradable particles, the degradation process was complete within the 24-hour time frame.

Improved elution profiles were seen with nanoparticles that were not fully degradable and that contained AMPS. However, the released KAFAK was susceptible to degradation. In the current studies, overall, more KAFAK was released from all nanoparticles in a serum environment as compared to the PBS only environment previously examined. This may indicate a competitive binding and release of serum proteins to facilitate KAFAK releases.

As shown in Figure 2 a dose dependent suppression in TNF-α expression by activated THP1 macrophages was achieved by varying the concentration of nanoparticles. The data also demonstrates, similar to what is seen in Figure 1, that degradable nanoparticles have a greater therapeutic effect due to increase in the amount of therapeutically available KAFAK.

Suppression of TNF-α expression has been previously shown to be an essential sign of down regulation of the pro-inflammatory cytokine cascade in macrophages. The ability of poly(NIPAm-co-AMPS) nanoparticles loaded with KAFAK to suppress TNF-α expression suggests that the therapeutic delivery strategy is able to attenuate this signaling cascade in macrophages.

In order to determine how nanoparticles would be distributed in OA-like environment we utilized a bovine knee cartilage plug model. Trypsinizing the cartilage matrix removes native aggrecan, but leaves hyaluronic acid and type II collagen intact, thus creating an unhealthy environment for chondrocytes. Diffusion of the nanoparticles, or KAFAK alone, into the plugs is depicted by an increase in the fluorescence intensity as shown in the images in Figure 3. When treated with KAFAK alone (Supplemental Figure 5) there was no selectivity for treatment of healthy tissue or damaged tissue. However, when healthy tissue was exposed to non-degradable nanoparticles loaded with KAFAK (Figure 3, normal tissue) very little KAFAK diffused into the healthy knee plugs. When degradable nanoparticles were tested (Figure 3, 5% DMHA) some nanoparticle degradation fragments with KAFAK and or free KAFAK released from DMHA degradable cross-linked particles was able to diffuse a short distance into the healthy cartilage. The average intensity values measured indicated no statistical significance between treatments given to a healthy tissue. However, **w**hen nanoparticles loaded with KAFAK were added to damaged cartilage plugs the nanoparticles were able to efficiently deliver KAFAK, diffusing from the top articular surface to the end deep zone. As shown in Figure 3, there is a significant difference in fluorescent intensity between healthy and damaged tissue. Damaged tissue treated with 5 and 10% AMPS show the highest average intensity. Overall, Figures 3 shows that KAFAK

poly(NIPAm-co-APS) is a promising therapeutic for specifically targeting the OA tissue. Although KAFAK showed non-specific diffusion into aggrecan free and normal tissue (Supplemental Figure 5), little to no diffusion of the nanoparticles was seen in healthy tissue but significant diffusion took place into damaged cartilage tissue.

Nanoparticles loaded with KAFAK were then used to determine the therapeutic efficacy of reducing pro-inflammatory cytokine production in an inflamed cartilage plug. Figure 4 demonstrates that after 2 days of IL-1B stimulated inflammation, KAFAK-loaded nanoparticles were able to reduce the production of IL-6 for a six-day culture period. Consistent with the results presented in Figure 2, particles containing DMHA were able to release more therapeutically active KAFAK quicker than particles containing MBA. However, a slight reduction in activity was seen in KAFAK released from DMHA over time most likely due to enzymatic degradation of unprotected KAFAK free in serum in the plug culture. This was confirmed by a lack of therapeutic activity between 2-day measurements of KAFAK alone and was consistent with the previously reported serum half-life of KAFAK being less than 12 hours.

Discussion

Traditionally nonsteroidal anti-inflammatory drugs, disease modifying anti-rheumatic drugs, corticosteroid therapy, and biologics have been used for treating osteoarthritis. Each therapy has potential drawbacks but all of them usually accompany significant side effects due to off target activity associated with unanticipated biological activity, and to systemic, rather than local drug activity. Biologics show great promise as treatment therapies. They currently comprise over 40% of the market, but their high cost and side effects provide significant opportunity for improved treatment options. In addition, delivery of therapies that target articular cartilage are limited by a tightly woven ECM of collagen fibers and proteoglycans. Correct tuning of nanoparticle size may be an essential requirement to modulate site-specific drug delivery *in vivo*. An important target size previously reported for nanoparticles is within 160nm–400nm. Particles within this size range show promise for selectively targeting tumor and inflamed tissue through leaky vasculature. Interarticular delivery of therapeutics into the synovial space is limited by a retention time less than 72 hours, where particles smaller than 5μm have been shown to be taken up by cells. In this and previous studies we have reported the ability to produce nanoparticles with sizes ranging between 100nm and 400nm in solution. With the ability to tune nanoparticles to a smaller range, we anticipate the treatment with poly(NIPAm-AMPS) nanoparticles will be able to enter cells, preventing diffusion out of the synovial fluid. KAFAK, released from either degradable or non-degradable systems, is effective at reducing cytokine production in both macrophages and cells within cartilage tissue (Figure 2 and 4). Reduction in TNF-α and IL-6 expression with KAFAK treatment indicates a suppression of MK2 kinase activity. Without these critical pro-inflammatory cytokines it is likely that the progression of osteoarthritis would be dampened with our therapy. The poly(NIPAm-co-AMPS) carrier has been previously shown to increase half-life of KAFAK in serum, and Figure 4 indicates that KAFAK delivered from nanoparticles is effective at reducing pro-inflammatory cytokine production during 2-day treatments.

Poly(NIPAm-co-AMPS) nanoparticles could be used through intra-articular injections into the synovial fluid of the knee. Figure 1 demonstrates that KAFAK releases rapidly from poly(NIPAm-co-AMPS) nanoparticles that are fully degradable in serum, but nanoparticles containing limited degradability and more AMPS tend to hold in more KAFAK over time. The results presented here demonstrate the release of KAFAK in *in vitro* and *ex vivo* experimental conditions where cell culture needed to be supplemented with FBS. Future experiments will examine the release of *KAFAK in vivo* models without serum supplementation.

Figure 2 indicates that the amount of KAFAK released from both degradable and non-degradable systems provides a therapeutically effective dose to reduce TNF-α production by macrophages during four days of treatment. Since macrophages play a principle role in perpetuating an inflammatory response, the suppression of inflammation in macrophages should enable a reduction in enzymatic degradation of inflamed tissue.

However, in order to better understand how cells within cartilage tissue would react to KAFAK treatment we stimulated bulk cartilage tissue with pro-inflammatory cytokines and then dosed with MK2-inhibiting KAFAK treatment. According to Figures 3 the targeting of only damaged tissue is possible with our sulfated carrier of anti-inflammatory peptide KAFAK. This passive targeting could provide an avenue for reduced system toxicity and a reduction in the amount of drug required for treatment. Table 1 indicates that KAFAK does not induce cell death in macrophages or chondrocytes, two key cell types involved in osteoarthritis pathogenesis and present in the synovial fluid and in cartilage tissue. The overall effect of passive targeting and reduced cellular toxicity is very promising for reduction of treatment side effects.

Overall we have demonstrated that KAFAK is an excellent treatment to reduce pro-inflammatory cytokine expression in macrophages and in bulk cartilage plugs. The *ex vivo* environment studied also provides evidence of selective targeting of larger charged nanoparticles into damaged tissue. Accordingly, a negative preference of diffusion into healthy cartilage was observed with KAFAK loaded nanoparticles. These promising results indicate that MK2 inhibitor KAFAK, when loaded into poly(NIPAm-co-AMPS) nanoparticles, can selectively and effectively reduce expression of pro-inflammatory cytokines within inflamed cartilage.

Supplementary Material

Refer to Web version on PubMed Central for supplementary material.

Acknowledgments

Support: Funding for this work came in part from HL106792.

References

1. Elaissari A. Thermally sensitive colloidal particles: From preparation to biomedical applications. Smart Colloidal Materials. 2006; 133:9–14. 184.

2. Dai S, Ravi P, Tam KC. Thermo- and photo-responsive polymeric systems. Soft Matter. 2009; 5(13):2513–33.
3. Lyon LA, Meng ZY, Singh N, Sorrell CD, John AS. Thermoresponsive microgel-based materials. Chemical Society Reviews. 2009; 38(4):865–74. [PubMed: 19421566]
4. Gu JX, Xia F, Wu Y, Qu XZ, Yang ZZ, Jiang L. Programmable delivery of hydrophilic drug using dually responsive hydrogel cages. Journal of Controlled Release. 2007; 117(3):396–402. [PubMed: 17239981]
5. Meng ZY, Cho JK, Debord S, Breedveld V, Lyon LA. Crystallization behavior of soft, attractive microgels. Journal of Physical Chemistry B. 2007; 111(25):6992–7.
6. Weissleder R, Kelly K, Sun EY, Shtatland T, Josephson L. Cell-specific targeting of nanoparticles by multivalent attachment of small molecules. Nat Biotechnol. 2005; 23(11):1418–23. Epub 2005/10/26. [PubMed: 16244656]
7. Garcia-Salinas MJ, Donald AM. Use of environmental scanning electron microscopy to image poly(N-isopropylacrylamide) microgel particles. J Colloid Interface Sci. 342(2):629–35. Epub 2009/12/08. [PubMed: 19962151]
8. Garcia-Salinas MJ, Romero-Cano MS, de las Nieves FJ. Colloidal stability of a temperature-sensitive Poly(N- isopropylacrylamide/2-acrylamido-2-methylpropanesulphonic acid) microgel. Journal of Colloid and Interface Science. 2002; 248(1):54–61. [PubMed: 16290503]
9. Garcia-Salinas MJ, Romero-Cano MS, de las Nieves FJ. Electrokinetic Characterization of Poly(N-isopropylacrylamide) Microgel Particles: Effect of Electrolyte Concentration and Temperature. J Colloid Interface Sci. 2001; 241(1):280–5. Epub 2001/08/15. [PubMed: 11502131]
10. Bartlett RL 2nd, Medow MR, Panitch A, Seal B. Hemocompatible poly(NIPAm-MBAAMPS) colloidal nanoparticles as carriers of anti-inflammatory cell penetrating peptides. Biomacromolecules. 2012; 13(4):1204–11. Epub 2012/03/29. [PubMed: 22452800]
11. Bartlett R, Panitch A. Thermosensitive nanoparticles with pH triggered degradation and release of anti-inflammatory cell penetrating peptide. Biomacromolecules [IN REVIEW]. 2012
12. Brugnano JL, Chan BK, Seal BL, Panitch A. Cell-penetrating peptides can confer biological function: Regulation of inflammatory cytokines in human monocytes by MK2 inhibitor peptides. Journal of Controlled Release. 2011; 155(2):128–33. [PubMed: 21600941]
13. Roux PP, Blenis J. ERK and p38 MAPK-activated protein kinases: a family of protein kinases with diverse biological functions. Microbiology and Molecular Biology Reviews. 2004; 68(2):320–+. [PubMed: 15187187]
14. Engel K, Ahlers A, Brach MA, Herrmann F, Gaestel M. Mapkap Kinase-2 Is Activated by Heat-Shock and Tnf-Alpha - in-Vivo Phosphorylation of Small Heat-Shock Protein Results from Stimulation of the Map Kinase Cascade. Journal of Cellular Biochemistry. 1995; 57(2):321–30. [PubMed: 7759569]
15. Belka C, Ahlers A, Sott C, Gaestel M, Herrmann F, Brach MA. Interleukin (Il)-6 Signaling Leads to Phosphorylation of the Small Heat-Shock Protein (Hsp)27 through Activation of the Map Kinase and Mapkap Kinase-2 Pathway in Monocytes and Monocytic Leukemia-Cells. Leukemia. 1995; 9(2):288–94. [PubMed: 7869766]
16. Arner EC, Hughes CE, Decicco CP, Caterson B, Tortorella MD. Cytokine-induced cartilage proteoglycan degradation is mediated by aggrecanase. Osteoarthritis and Cartilage. 1998; 6(3): 214–28. [PubMed: 9682788]
17. Neininger A, Kontoyiannis D, Kotlyarov A, Winzen R, Eckert R, Volk HD, et al. MK2 targets AU-rich elements and regulates biosynthesis of tumor necrosis factor and interleukin-6 independently at different post-transcriptional levels. Journal of Biological Chemistry. 2002; 277(5):3065–8. [PubMed: 11741878]
18. McInnes IB, Schett G. Cytokines in the pathogenesis of rheumatoid arthritis. Nature Reviews Immunology. 2007; 7(6):429–42.
19. Pelletier JP, Martel-Pelletier J, Abramson SB. Osteoarthritis, an inflammatory disease - Potential implication for the selection of new therapeutic targets. Arthritis and Rheumatism. 2001; 44(6): 1237–47. [PubMed: 11407681]

20. Pratta MA, Yao WQ, Decicco C, Tortorella MD, Liu RQ, Copeland RA, et al. Aggrecan protects cartilage collagen from proteolytic cleavage. Journal of Biological Chemistry. 2003; 278(46): 45539–45. [PubMed: 12890681]
21. Arner EC, Pratta MA, Decicco CP, Xue CB, Newton RC, Trzaskos JM, et al. Aggrecanase - A target for the design of inhibitors of cartilage degradation. Inhibition of Matrix Metalloproteinases: Therapeutic Applications. 1999; 878:92–107.
22. Pratta MA, Dimeo TM, Ruhl DM, Arner EC. Effect of Interleukin-1-Beta and Tumor Necrosis Factor-Alpha on Cartilage Proteoglycan Metabolism Invitro. Agents and Actions. 1989; 27(3–4): 250–3. [PubMed: 2801305]
23. Ulbrich K, Subr V, Seymour LW, Duncan R. Novel Biodegradable Hydrogels Prepared Using the Divinylic Cross-Linking Agent N,O-Dimethacryloylhydroxylamine .1. Synthesis and Characterization of Rates of Gel Degradation, and Rate of Release of Model-Drugs, Invitro and Invivo. Journal of Controlled Release. 1993; 24(1–3):181–90.
24. Ulbrich K, Subr V, Podperova P, Buresova M. Synthesis of Novel Hydrolytically Degradable Hydrogels for Controlled Drug-Release. Journal of Controlled Release. 1995; 34(2):155–65.
25. Gan DJ, Lyon LA. Tunable swelling kinetics in core-shell hydrogel nanoparticles. Journal of the American Chemical Society. 2001; 123(31):7511–7. [PubMed: 11480971]
26. Hu ZB, Huang G. A new route to crystalline hydrogels, guided by a phase diagram. Angewandte Chemie-International Edition. 2003; 42(39):4799–802.
27. Niikura T, Reddi AH. Differential regulation of lubricin/superficial zone protein by transforming growth factor beta/bone morphogenetic protein superfamily members in articular chondrocytes and synoviocytes. Arthritis and rheumatism. 2007; 56(7):2312–21. Epub 2007/06/30. [PubMed: 17599751]
28. Poole AR, Pidoux I, Reiner A, Tang LH, Choi H, Rosenberg L. Localization of Proteoglycan Monomer and Link Protein in the Matrix of Bovine Articular-Cartilage - an Immunohistochemical Study. Journal of Histochemistry & Cytochemistry. 1980; 28(7):621–35. [PubMed: 6156200]
29. Eigler A, Sinha B, Hartmann G, Endres S. Taming TNF: strategies to restrain this proinflammatory cytokine. Immunology Today. 1997; 18(10):487–92. [PubMed: 9357141]
30. Kinne RW, Stuhlmuller B, Burmester GR. Cells of the synovium in rheumatoid arthritis - Macrophages. Arthritis Research & Therapy. 2007; 9(6)
31. Kalb RE, Strober B, Weinstein G, Lebwohl M. Methotrexate and psoriasis: 2009 National Psoriasis Foundation Consensus Conference. Journal of the American Academy of Dermatology. 2009; 60(5):824–37. [PubMed: 19389524]
32. Sokolovic S. Corticosteroid therapy and atherosclerosis risk in rheumatoid arthritis patients. Clinical and Experimental Rheumatology. 2009; 27(5):717.
33. Kwoh CK, Anderson LG, Greene JM, Johnson DA, O'Dell R, Robbins ML, et al. Guidelines for the management of rheumatoid arthritis - 2002 update. Arthritis and Rheumatism. 2002; 46(2): 328–46. [PubMed: 11840435]
34. Stoll JG, Yasothan U. Rheumatoid arthritis market. Nature Reviews Drug Discovery. 2009; 8(9): 693–4.
35. Hoebert JM, Mantel-Teeuwisse AK, van Dijk L, Bijlsma JW, Leufkens HG. Do rheumatoid arthritis patients have equal access to treatment with new medicines?: tumour necrosis factor-alpha inhibitors use in four European countries. Health Policy. 104(1):76–83. Epub 2011/11/15. [PubMed: 22079753]
36. Comper, WD. Physicochemical aspects of cartilage extracellular matrix. In: Hall, B.; Newman, S., editors. Cartilage: Molecular Aspects. CRC Press; Boston: 1991. p. 59-96.
37. O'Neal DP, Hirsch LR, Halas NJ, Payne JD, West JL. Photo-thermal tumor ablation in mice using near infrared-absorbing nanoparticles. Cancer Lett. 2004; 209(2):171–6. Epub 2004/05/26. [PubMed: 15159019]
38. Sandanaraj BS, Gremlich HU, Kneuer R, Dawson J, Wacha S. Fluorescent nanoprobes as a biomarker for increased vascular permeability: implications in diagnosis and treatment of cancer and inflammation. Bioconjug Chem. 21(1):93–101. Epub 2009/12/05. [PubMed: 19958018]
39. Gerwin N, Hops C, Lucke A. Intraarticular drug delivery in osteoarthritis. Advanced drug delivery reviews. 2006; 58(2):226–42. Epub 2006/04/01. [PubMed: 16574267]

40. Ratcliffe JH, Hunneyball IM, Smith A, Wilson CG, Davis SS. Preparation and evaluation of biodegradable polymeric systems for the intra-articular delivery of drugs. The Journal of pharmacy and pharmacology. 1984; 36(7):431–6. Epub 1984/07/01. [PubMed: 6146685]

41. Owen SG, Francis HW, Roberts MS. Disappearance kinetics of solutes from synovial fluid after intra-articular injection. British journal of clinical pharmacology. 1994; 38(4):349–55. Epub 1994/10/01. [PubMed: 7833225]

42. Bartlett RL 2nd, Panitch A. Thermosensitive Nanoparticles with pH-Triggered Degradation and Release of Anti-inflammatory Cell-Penetrating Peptides. Biomacromolecules. 2012; 13(8):2578–84. Epub 2012/08/03. [PubMed: 22852804]

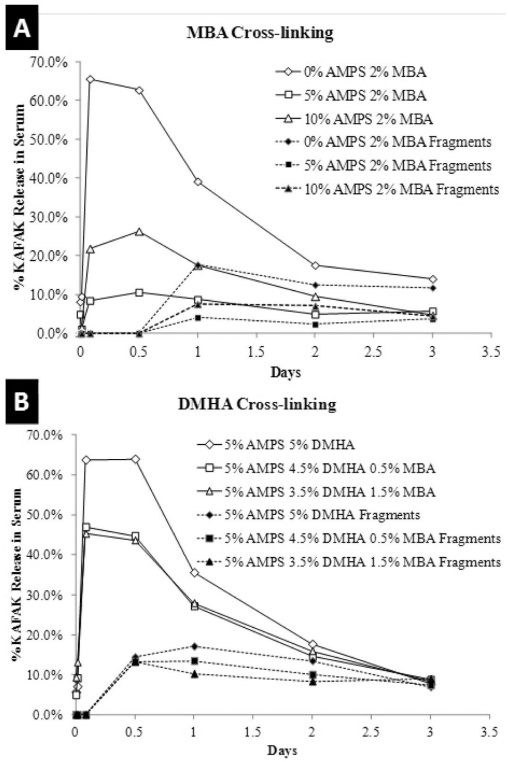

Figure 1.

Percent of loaded KAFAK released in 10% FBS PBS solution at 37°C. A) MBA cross-linked only nanoparticles. B) DMHA only or DMHA and MBA cross-linked nanoparticles. Lines represent data from two sample sets.

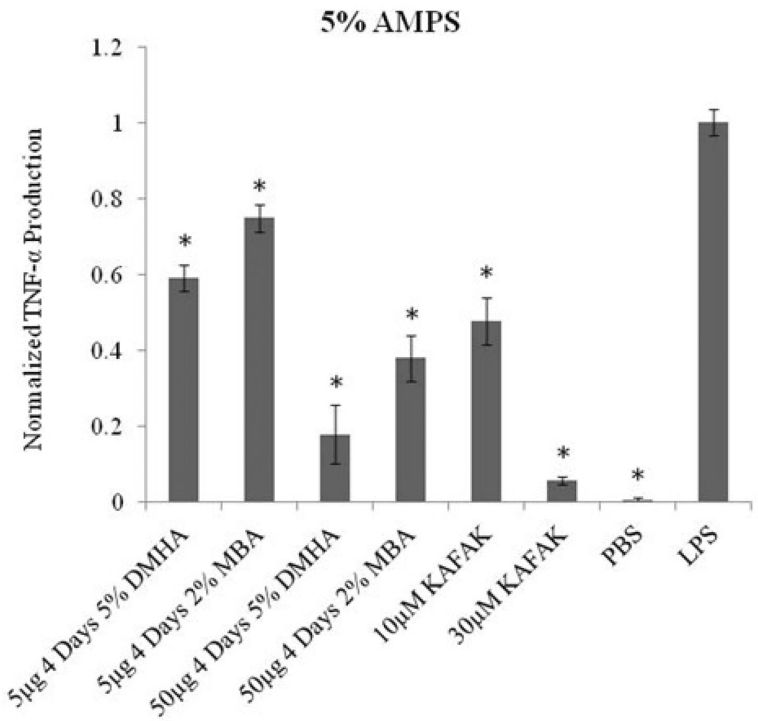

Figure 2.

TNF-α production in THP1 human macrophage model treated with different concentrations of DMHA, MBA and KAFAK. Positive and negative controls are represented as treatment with PBS and LPS respectively. Bars represent average±SEM (N=4). * denotes statistical significance ($p<0.05$) between treatment groups and LPS.

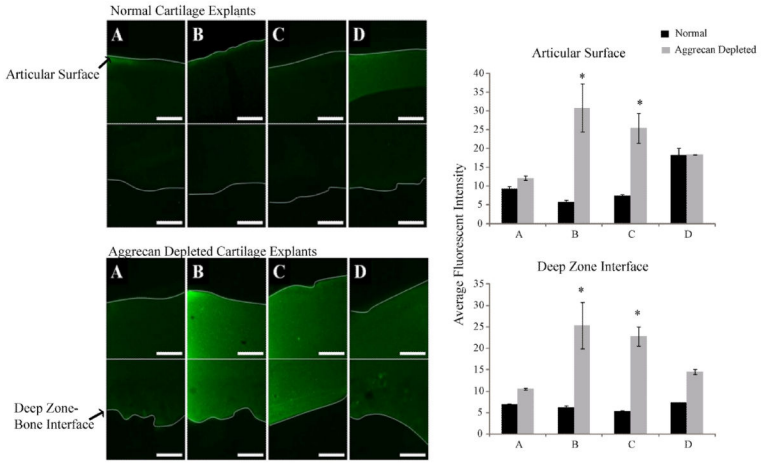

Figure 3.

Saggital cross sectional area of load bearing region of bovine knee explants representing articular surface (cartilage-synovial fluid interface) to the deep zone (bone-cartilage interface) taken with 488 nm excitation of FITC-labeled KAFAK in nanoparticles (Scale is 50μm). First panel represents normal healthy cartilage. Second panel represents aggrecan depleted cartilage explants. A) KAFAK in 0% AMPS 2% MBA nanoparticles in normal tissue. B) KAFAK in 5% AMPS 2% MBA nanoparticles in normal tissue. C) KAFAK in 10% AMPS 2% MBA nanoparticles in normal tissue. D) KAFAK in 5% AMPS 5% DMHA nanoparticles in normal tissue. Average intensity values indicate a significantly higher value seen in aggrecan depleted cartilage treated with 5% AMPS and 10% AMPS as compared to the other treatments. Significance denoted as *($p<0.001$). Bars represent average±SEM (N=3).

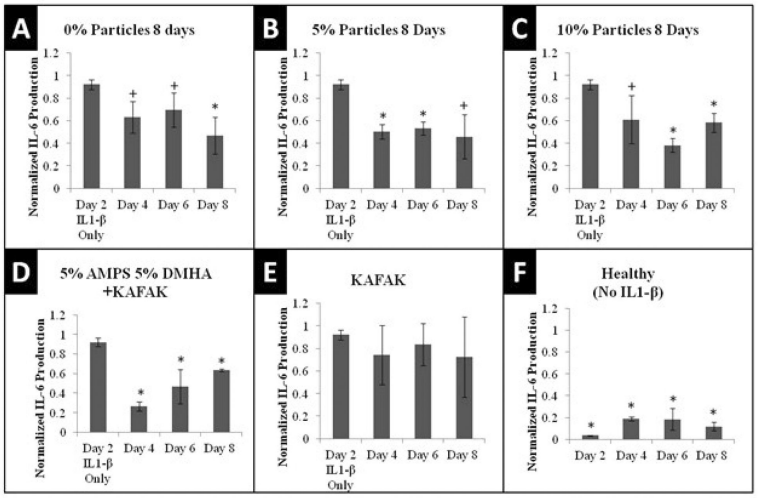

Figure 4.

IL-6 Production in Cartilage Plugs when dosed with 50μg nanoparticles loaded with KAFAK. Plots A–E represents aggrecan depleted plugs dosed with IL-1β. Plot F represents plugs with intact aggrecan and no IL-1β stimulation. Plots are normalized to individual plug weight and IL-6 production from the negative control and represent average ± SEM (N=4). *P<.05 or $0.05<^{+}P<0.10$ with respect to IL-1β only treatment

Table 1

Nanoparticle Cross linking Composition*

Mole % AMPS	**0%**	**5%**	**10%**	**5%**	**5%**	**5%**
Mole % MBA	2%	2%	2%	0%	0.5%	1.5%
Mole % DMHA	0%	0%	0%	5%	4.5%	3.5%

Table 2

Poly(NIP Am-AMPS) Nanoparticle Properties

Composition	0 % AMPS 2 % MBA	5 % AMPS 2 % MBA	10 % AMPS 2 % MBA	5 % AMPS 5 % DMHA
Drug Loading by weight[10, 11]	17.8 ± 7.1%	45.3 ± 9.5 %	60.5 ± 6.2 %	24.30 ± 4.10%
Zeta Potential[10, 11]	−6.1 ± 0.9mv	−13.6 ± 1.4 mv	−22.9 ± 3.3 mv	−15.6 ± 1.7 mv
Diameter at 23°C[10, 11]	293.2 ± 10.0 nm	315.1 ± 17.4 nm	358.1 ± 52.1 nm	408.2 ± 6.6 nm
Diameter at 37°C[10, 11]	129.1 ± 10.5 nm	222.6 ± 14.5 nm	288.3 ± 49.8 nm	232.5 ± 4.7 nm